Nuclear Physics B102 (1976) 120–138

A CORRELATED JET MODEL DESCRIPTION OF THE REACTION $\pi^+ p \to p 3\pi^+ 2\pi^-$ AT 8 AND 16 GeV/c

K.J. BIEBL, M. KLEIN, R. NAHNHAUER and H. SCHILLER
Institut für Hochenergiephysik, Akademie der Wissenschaften der DDR, Berlin-Zeuthen

Received 30 June 1975
(Revised 13 October 1975)

A correlated jet model which takes into account dynamical two-particle correlations besides exact kinematical ones is compared with data of the reaction $\pi^+ p \to p 3\pi^+ 2\pi^-$. The approximation of the dynamical correlation by the contributions of the resonances ρ^0, Δ^{++} and Δ^0 is shown to yield a good description of single-, two- and three-particle distributions. Short-range effects of two-pion azimuthal angular correlations are explained mainly by the decay of ρ^0 being produced with limited transverse momentum.

1. Introduction

Recent experimental results for correlations in high energy inclusive and semi-inclusive reactions [1] indicate that there is a strong short-range component in the central region. This has been considered as an evidence for the production of clusters which may be regarded as excited hadronic states decaying into the observed final state particles. There are two leading clusters (or particles) [2] which carry mostly the quantum numbers of the two incoming particles and a varying number of central clusters produced almost independently.

Various cluster models have been constructed [1] which differ by the assumptions for the mechanism of cluster production (e.g. multiperipheral, independent emission) and cluster decay (e.g. independent emission with invariant phase space, thermodynamic fireball decay, resonant decay). Most of these models neglect energy momentum conservation which is permissible only in the central region at asymptotic energies.

In this paper we want to compare the data for the reaction $\pi^+ p \to p 3\pi^+ 2\pi^-$ at 16 and 8 GeV/c with a correlated jet model (CJM) considered by one of us [3] * as a combination of the uncorrelated jet model (UJM) [4] and the Feynman gas model (FGM) [5, 6]. In the special form used here it may be regarded as belonging to the general class of cluster models mentioned. Energy-momentum conservation is taken

* A model of this type has been used already in ref. [14] for the investigation of the high-energy behaviour of the total cross section and of multiplicity moments.

into account exactly as in the UJM including δ functions in all exclusive cross sections. This exact treatment of kinematics of the final state particles (phase space) is always important for the distributions of particles in the fragmentation regions. At non-asymptotic energies kinematical effects can be considerable [1] also in the central region, especially if it extends only over a few rapidity units, even more for energies below 50 GeV/c.

For the dynamics, i.e. for the invariant matrix elements squared, $|T_n(p_1, ..., p_n)|^2$, we assume in a first approximation the factorization structure of the Feynman gas model (proposed originally for the cross sections); thus $|T_n|^2$ consists of a sum of products of the functions $\varphi_1(p_i)$ and $\varphi_2(p_i, p_j)$. Here $\varphi_1(p_i)$ describes the production of a "one-particle cluster", i.e. the final state particle itself, produced with momentum p_i, and $\varphi_2(p_i, p_j)$ represents the production of a two-particle cluster of momentum $p_i + p_j$ which decays into the two stable particles of momenta p_i and p_j. Higher order correlation functions $\varphi_m(p_1, ..., p_m)$ of $|T_n|^2$ are not included here since two-particle correlations seem to be dominant, at least in this low-energy reaction. Leading particle effects, however, are taken into account by using different functions ψ^a_m and ψ^b_m for the leading forward (a) and backward (b) particles and clusters instead of the central cluster functions φ_m.

The main physical reason for the presence of the correlation φ_2 in $|T_n|^2$ is the strong production of resonances in the low-mass region, $M^2_{ij} = (p_i + p_j)^2$. They are assumed here to have a transversal cutoff in the net transversal momentum $(p_i + p_j)_\perp$, (or, more appropriately, in the longitudinal mass $\mu^2_{ij} = M^2_{ij} + (p_i + p_j)^2_\perp$), similar to the transversal cutoff used for φ_1 in the UJM, and a Breit-Wigner type function in M^2_{ij} for the propagation and decay of the resonance. In this resonance approximation for φ_2 we have then a generalized jet model for the independent production of stable particles, e.g. pions, and of resonances, e.g. $\rho \to \pi + \pi$, two pions being correlated dynamically only if they come from the decay of the same ρ meson [7]. In general φ_2 can account also for more general dynamical two-particle correlations. In addition, the kinematical correlations are included automatically because of the δ functions.

Although such a model is intended mainly to be the basis for the calculation of the non-diffractive part of m-particle distributions in inclusive and semi-inclusive reactions we apply it here to an exclusive channel which has strong two-particle resonance production, in order to determine the two phenomenological functions φ_1 and φ_2, assuming φ_3 *etc.* to be small. We find that, even with the oversimplified resonance approximation for φ_2, one- and two-particle distributions are well represented, including the short-range effect in the azimuthal correlations of the $\pi^+\pi^-$ pair due to the ρ^0 resonance, and that in three-particle distributions, like $\pi^+\pi^+\pi^-$, an important part in the A resonance region comes from the uncorrelated $\pi^+\rho^0$ production.

2. The correlated jet model

2.1. General properties

For an exclusive reaction

$$a + b \to c_1 + \ldots + c_n \,, \tag{2.1}$$

the cross section has (up to the flux factor) the general form

$$d\sigma_n = \frac{1}{n!} \int dp_1 \ldots dp_n \, \delta^4 \left(P - \sum p_i \right) |T_n(p_1, \ldots, p_n)|^2 \,, \tag{2.2}$$

where $dp = d^3p/E$ and $P = p_a + p_b$. In the UJM the $|T_n|^2$ are assumed to factorize completely,

$$|T_n|^2 = \prod_{i=1}^{n} \varphi_1(p_i) \,. \tag{2.3}$$

If we want to take into account two-particle correlations in $|T_n|^2$ we have to use instead of (2.3)

$$\begin{aligned} |T_n(p_1, \ldots, p_n)|^2 &= \varphi_1(p_1) \cdot \ldots \cdot \varphi_1(p_n) \\ &+ \sum \varphi_2(p_1, p_2) \cdot \varphi_1(p_3) \cdot \ldots \cdot \varphi_1(p_n) \\ &+ \sum \varphi_2(p_1, p_2) \cdot \varphi_2(p_3, p_4) \cdot \varphi_1(p_5) \cdot \ldots \cdot \varphi_1(p_n) \\ &+ \ldots \,, \end{aligned} \tag{2.4}$$

where the summation extends over all permutations P of the momenta $p_1, \ldots, p_n$ which do not yield identical terms, i.e. we have to replace in all possible ways pairs of functions $\varphi_1(p_i), \varphi_1(p_j)$ in (2.3) by the "dynamical" correlation function $\varphi_2(p_i, p_j)$. More precisely, the expression for $|T_n|^2$ is determined by the recursion relation

$$\begin{aligned} |T_n(p_1, \ldots, p_n)|^2 &= |T_{n-1}(p_1, \ldots, p_{n-1})|^2 \cdot \varphi_1(p_n) \\ &+ \sum_{i=1}^{n-1} |T_{n-2}(p_1, \ldots, p_{i-1}, p_{i+1}, \ldots p_{n-1})|^2 \varphi_2(p_i, p_n) \,, \end{aligned} \tag{2.5}$$

where (formally) $|T_0|^2 = 1$ and $|T_1(p_1)|^2 = \varphi_1(p_1)$. Relations of this type for exclusive cross sections are known from the FGM [6]. We use them here, however, for the amplitude squared in (2.2). Therefore we have a Feynman gas model with energy

momentum conservation which takes into account both all kinematical correlations due to the δ functions in (2.2) and second-order dynamical correlations due to the φ_2 functions. Note that φ_2 describes both the production and decay of the clusters. In eq. (2.4) we have with one factor φ_2 also arbitrary powers of φ_2, i.e. an independent multiple production of the same cluster. Moreover, there is a full permutation symmetry of all particles. All this reflects general well-known structures of $|T_n|^2$, e.g. if there is a two-particle resonance in one subchannel (i, j) there must be also the same resonance in all other non-overlapping subchannels.

If we take into account higher order correlation functions φ_m, $m \geqslant 3$, we are dealing with a general correlation analysis of $|T_n|^2$, i.e. a search for factorizing or partially factorizing terms in $|T_n|^2$, beyond any specific cluster model. Here we want to use, however, in a first approximation only the Feynman gas formula (2.4) in order to study the effects of the lowest non-trivial dynamical correlations.

As in the UJM ($\varphi_2 = 0$) we have to expect that an independent multiple production of only one- and two-particle clusters holds only for newly produced central clusters. There are additionally two leading objects [2] which are the slightly deflected throughgoing particles or excitations of them. These leading particles ($m = 1$) or clusters ($m > 1$) must be described by different functions $\psi^{\mathrm{a}}_m(p_1, ..., p_m)$ and $\psi^{\mathrm{b}}_m(p_1, ..., p_m)$. The leading particle character, i.e. the "correlation" with the two incoming particles a and b, respectively, is represented by a momentum dependence different from that of the central cluster functions φ_m. In particular, these functions should become very small if the rapidity of the leading clusters is very different from the rapidities of a and b, respectively, whereas we have to assume a uniform rapidity distribution for the central clusters [4] ("leading" does not mean here, of course, that these particles have the biggest and smallest rapidity of all particles produced in each event, but that this configuration is dominant). Since we have only one leading forward cluster (a) and one leading backward cluster (b) each of the two functions ψ^{a}_m and ψ^{b}_m have to replace only one φ_m function in (2.4) in all possible ways, (see eq. (2.7) below).

The single-particle distribution calculated from (2.4) or its leading particle modification consists of two parts. In the first one the observed particle is singly produced (φ_1 or ψ_1), whereas in the second part it arises from the decay of a two-particle cluster (φ_2 or ψ_2). Similarly, in the two-particle distribution we have four parts, where the two observed particles are produced independently coming from two different "one"- and/or two-particle clusters, and a last part where both particles are the decay products of the same cluster. If we have e.g. a resonance in φ_2 or ψ_2 then this last part leads directly to the resonant structure of the two-particle distribution whereas the background of the first four parts contains besides the purely uncorrelated production also all "refections of resonances".

Although general properties of $|T_n|^2$ and of inclusive cross sections theoretically give restrictions for the functions φ_m, the CJM should be regarded not only as a phenomenological model with almost arbitrary functions φ_m but also as a convenient frame for the correlation analysis of multi-particle production data.

2.2. Specification for the reaction $\pi^+p \to p3\pi^+2\pi^-$

Since the correlated jet model is mainly intended to describe the non-diffractive and especially the central part of the amplitude, the multiplicity of the studied exclusive reaction should not be too small. Furthermore one should choose for the first comparison of the model with experimental data a reaction channel with exactly measured energy and momentum of all produced particles and high statistics for the determination of the energy independent model parameters. So we studied the reaction

$$\pi^+\mathrm{p} \to \mathrm{p}3\pi^+2\pi^- \tag{2.6}$$

at 16 GeV/c with 5023 events and at 8 GeV/c with 530 events in which according to ref. [9] mainly two-particle resonances (ρ, Δ) are produced.

In this section we give the detailed formulae for the exclusive cross section of (2.6) as they follow from the leading particle modification of (2.5).

The amplitude squared consists of six terms f_i with special leading particles or two-particle clusters neglecting the leading π^- because of the smallness of double charge exchange. In a symbolic notation and keeping in mind the permutations necessary (2.4) we have

$$f_1 = \sum \psi_1^{\mathrm{a}}(\pi^+)\psi_1^{\mathrm{b}}(\mathrm{p})\,[\varphi_1^2(\pi^+)\varphi_1^2(\pi^-) + \varphi_1(\pi^+)\varphi_1(\pi^-)\varphi_2(\pi^+\pi^-) + \varphi_2^2(\pi^+\pi^-)]\,,$$

$$f_2 = \sum \psi_2^{\mathrm{a}}(\pi^+\pi^-)\psi_1^{\mathrm{b}}(\mathrm{p})\,[\varphi_1^2(\pi^+)\varphi_1(\pi^-) + \varphi_1(\pi^+)\varphi_2(\pi^+\pi^-)]\,,$$

$$f_3 = \sum \psi_1^{\mathrm{a}}(\pi^+)\,\psi_2^{\mathrm{b}}(\mathrm{p}\pi^+)\,[\varphi_1(\pi^+)\varphi_2^2(\pi^-) + \varphi_1(\pi^-)\varphi_2(\pi^+\pi^-)]\,,$$

$$f_4 = \sum \psi_2^{\mathrm{a}}(\pi^+\pi^-)\,\psi_2^{\mathrm{b}}(\mathrm{p}\pi^+)\,[\varphi_1(\pi^+)\varphi_1(\pi^-) + \varphi_2(\pi^+\pi^-)]\,,$$

$$f_5 = \sum \psi_1^{\mathrm{a}}(\pi^+)\,\psi_2^{\mathrm{b}}(\mathrm{p}\pi^-)\,[\varphi_1^2(\pi^+)\varphi_1(\pi^-) + \varphi_1(\pi^+)\varphi_2(\pi^+\pi^-)]\,,$$

$$f_6 = \sum \psi_2^{\mathrm{a}}(\pi^+\pi^-)\,\psi_2^{\mathrm{b}}(\mathrm{p}\pi^-)\varphi_1^2(\pi^+)\,, \tag{2.7}$$

with

$$|T|^2 = \sum_{i=1}^{6} f_i\,. \tag{2.8}$$

It should be noticed that in the considered approximation for correlations including

only resonances, the functions φ_2 and ψ_2 for the exotic combinations $(\pi^+\pi^+)$ and $(\pi^-\pi^-)$ are assumed to be zero.

For choosing explicit expressions for the functions φ_m their relations to the inclusive distributions in the central region and their Mueller analysis suggest as the simplest choice that $\varphi_1(p)$ depends only on the longitudinal mass $\mu^2 = p_\perp^2 + m^2$ and $\varphi_2(p_1, p_2)$ in the resonance approximation on $m_{12}^2 = (p_1 + p_2)^2$ and $\mu_{12}^2 = (p_{1\perp} + p_{2\perp})^2 + m_{12}^2$. The dual model [8] suggests to take the transversal cutoff as a cutoff in the longitudinal masses. For simplicity we take here the gaussian form $\exp(-a\mu^2)$. Then we have

$$\varphi_1 = c_1 \exp(a\mu^2), \qquad \varphi_2 = c_2 \exp(a\mu^2_{\pi^+\pi^-}) \cdot b(\pi^+\pi^-). \tag{2.9}$$

Here $b(i, j)$ is a Breit-Wigner function

$$b(i,j) = \frac{m_0 \Gamma_0 \dfrac{q^{2l}}{q_0^{2l+1}}}{(m_{ij}^2 - m_0^2)^2 + \left(m_0 \Gamma_0 \left(\dfrac{q}{q_0}\right)^{2l+1}\right)^2}, \tag{2.10}$$

with

$$q = \frac{1}{2m_{ij}} \sqrt{(m_{ij}^2 - (m_i - m_j)^2)\,(m_{ij}^2 - (m_i + m_j)^2)},$$

$q_0 = q(m_{ij} = m_0)$, Γ_0 is the half-width of the resonance, l is the relative orbital angular momentum of the particles i and j. Notice that polarization effects of resonances are neglected.

In φ_2 the cutoff in the net transversal momentum $p_{1\perp} + p_{2\perp}$ of the cluster, which is strictly valid at the resonance pole, is responsible for many effects. In particular, pions coming from the same resonance ρ are most probably produced with opposite transversal momenta $p_{1\perp} = -p_{2\perp}$. This implies strong short range azimuthal correlations. The functions φ_m of the central part C must be energy independent in order to get scaling behaviour at asymptotic energies.

The leading particles or clusters are correlated with the incident particles a or b by the functions ψ_m which have an additional cutoff in the momentum transfer t_i^a or t_i^b, respectively. Thus the functions ψ_m are

$$\psi_1^b(\mathrm{p}) = \beta_\mathrm{p} \exp(d_1 t_\mathrm{p}^b + e_1 \mu^2),$$

$$\psi_1^a(\pi^+) = \beta_{\pi^+} \exp(d_2 t_{\pi^+}^a + e_2 \mu^2),$$

$$\psi_2^a(\pi^+\pi^-) = \beta_{\pi^+\pi^-} \exp(d_2 t_{\pi^+\pi^-}^a + e_2 \mu^2_{\pi^+\pi^-}) \cdot b(\pi^+\pi^-),$$

$$\psi_2^b(\mathrm{p}\pi^+) = \beta_{\mathrm{p}\pi^+} \exp(d_3 t_{\mathrm{p}\pi^+}^b + e_3 \mu^2_{\mathrm{p}\pi^+}) \cdot b(p\pi^+),$$

$$\psi_2^b(\mathrm{p}\pi^-) = \beta_{\mathrm{p}\pi^-} \exp(d_3 t_{\mathrm{p}\pi^-}^b + e_3\, \mu^2_{\mathrm{p}\pi^-}) \cdot b(p\pi^-). \tag{2.11}$$

Setting $c_1 = 1$ (the whole expression is only determined up to an overall factor) and inserting the expressions (2.9) and (2.11) into (2.7) we get with

$$\alpha_1 = \beta_\pi + \beta_p\,, \qquad \alpha_2 = \beta_{\pi^+\pi^-} \cdot \beta_p\,, \ldots, \qquad \alpha_6 = \beta_{\pi^+\pi^-} \cdot \beta_{p\pi^-}\,,$$

four independent parameters α, e.g.

$$\alpha_1, \alpha_2, \alpha_3, \alpha_5 \quad \text{and } \alpha_4 = \alpha_3\alpha_2/\alpha_1\,, \qquad \alpha_6 = \alpha_5\alpha_2/\alpha_1\,. \tag{2.12}$$

We define

$$g_i = f_i/\alpha_i\,, \quad i = 1, 2, \ldots, 6\,. \tag{2.13}$$

Hence (2.8)

$$|T|^2 = \sum_{i=1}^{6} \alpha_i g_i\,. \tag{2.14}$$

The parameters α_i are a measure for the probability of competing final states with defined leading particles or leading resonances; c_2/c_1^2 is a measure for the ratio of correlated to uncorrelated production in the central part.

3. Results of model calculations and comparison with the data

3.1. Fit of the CJM to the data

The phase-space integrations for the amplitude (2.8) were performed with the Monte-Carlo technique [10]. The cutoff parameters of the leading functions $\psi_m^{a,b}$, e_i and d_i, on which $|T|^2$ depends exponentially, were only roughly determined by comparing the theoretical with the experimental mean values for Feynman x and $p_\perp^2$ distributions (table 1). Moreover the parameter a of the functions φ_m has been fixed to be $-4.0\ (\mathrm{GeV}/c)^{-2}$ as usual.

On the other hand the parameters c_2 and β_i entering $|T|^2$ as polynominals were calculated by a χ^2 fit of the model curves to all two-particle mass distributions.

The results of the calculations at 16 GeV/c are given for some one- and two-particle distributions in figs. 1, 2 and 3. In general the experimental distributions are well described by the CJM curves. Figs. 1a, 1b, and 1c show the Feynman x distributions of p, π^+, and π^-. Small deviations between the theoretical and the experimental curves might be attributed to the chosen t cutoff parameters. The $p_\perp^2$ distributions (fig. 2) are very well described by the model curves in a region up to $p_\perp^2 \sim 0.5\ (\mathrm{GeV}/c)^2$.

Fig. 3 shows two-particle mass distributions which are also well represented by the correlated jet model. For comparison we also have included as dashed curves the results from the uncorrelated jet model, i.e. $|T|^2$ (2.8) with $\varphi_2 = 0$ and all $\psi_2^{a,b} = 0$. These curves are normalized here, however, to the tail of the $\pi^+\pi^-$ mass distributions; actually in the CJM this term is smaller by a factor $\frac{1}{7}$.

Table 1
Model parameters at 8 and 16 GeV/c lab momentum in $[\mathrm{GeV}/c]^{-2}$

P_{LAB}	a	e_1	e_2	e_3	d_1	d_2	d_3
8GeV/c	- 4.0	-1.5	-3.0	-1.5	0.3	0.05	0.1
16 GeV/c					1.3	0.1	0.3

$$m_{\rho^0} = 765\ \mathrm{MeV};\ \Gamma_{\rho^0} = 135\ \mathrm{MeV};\ l_{\rho^0} = 1$$

$$m_{\Delta} = 1236\ \mathrm{MeV};\ \Gamma_{\Delta} = 120\ \mathrm{MeV};\ l_{\Delta} = 1$$

$$C_2 = 0.88 \pm 0.11$$

The CJM was applied to the same reaction (2.6) at 8 GeV/c in order to study the energy dependence of the model amplitude squared. The parameters e_i and d_i involved in the functions $\psi_m^{a,b}$ for the leading objects are determined in the same manner as at 16 GeV/c. We find that the μ cutoff parameters e_i are roughly constant whereas the parameters d_i which determine the strength of the t cutoff are smaller at 8 GeV/c (table 1). This means that the leading particles at lower energies are less distinguishable from the particles centrally produced. At least for the proton it is in agreement with the general Regge behaviour of the slope parameter.

On the other hand the central part of the amplitude squared is assumed to be energy independent (see subsect. 2.2). Therefore we used the same functions φ_m as at 16 GeV/c. With this assumption we find that the experimental distributions at 8 GeV/c, e.g. the two-particle mass distributions given in fig. 4 are represented by the CJM as well as those at 16 GeV/c.

3.2. Estimation of resonance production

It is one of the purposes of the CJM to yield a reasonable description of the resonance production. The fit can be performed on the level of the amplitude squared instead of the cross section.

The full permutation symmetry of $|T|^2$ implies that resonances appear in all relevant two-particle subsystems. So, by construction, any two-particle distribution

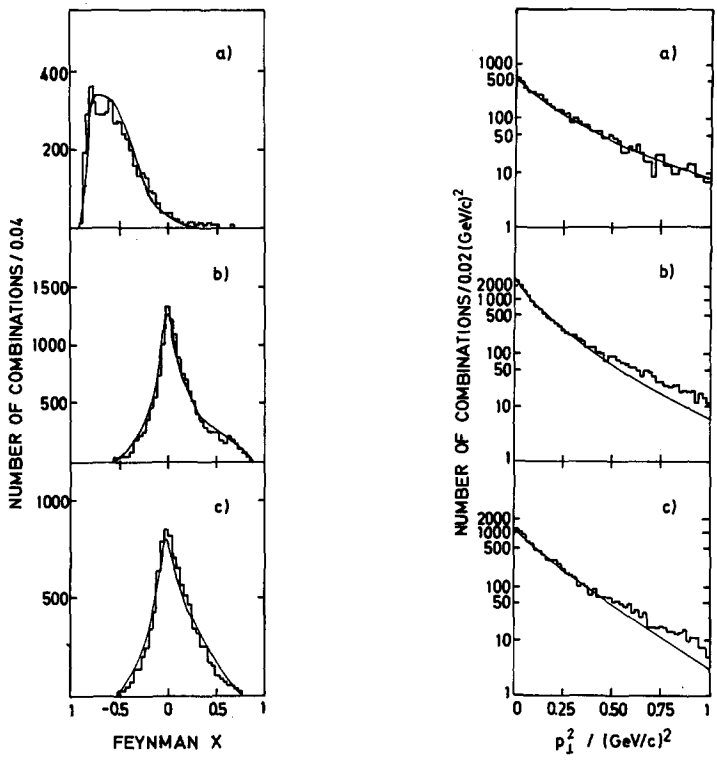

Fig. 1. Feynman x distribution for p, π^+, π^- at 16 GeV/c and CJM curve.

Fig. 2. Squared transverse momentum distribution for p, π^+, π^- at 16 GeV/c and CJM curve.

contains also all contributions which are reflections of other resonances.

In order to investigate this in more detail we decompose the terms f_i (eq. 2.14) according to their different central ρ^0 content arriving altogether at 12 different terms. They are denoted by "(leading forward object/central objects/leading backward object)". Their relative amounts (table 2) which are determined by the parameters α_i and c_2 fitted simultaneously to all two-particle mass distributions are a measure for the appearance of competing reaction channels and give the possibility to estimate the relative contributions of pure uncorrelated production and resonance production.

These values are quite similar for 8 and 16 GeV/c and coincide within the errors with those obtained by Böttcher et al. [9] having used the LPS method (table 3). We find that in 12% of all events we have pure uncorrelated production (table 2.).

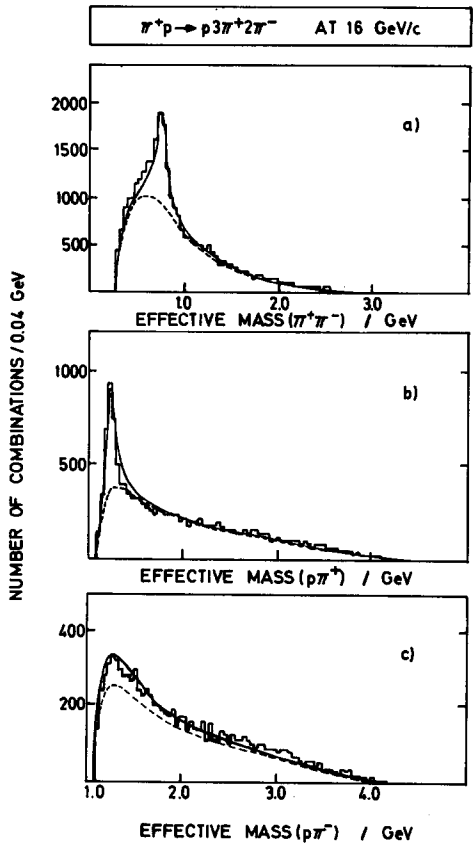

Fig. 3. Two-particle mass distribution for $(\pi^+\pi^-)$, $(p\pi^+)$, $(p\pi^-)$ at 16 GeV/c. Solid curve: CJM; dashed curve: UJM normalized to the tails of the experimental $(\pi^+\pi^-)$ distribution.

In contrast to the small Δ^0 contribution of 1–2% we have a strong Δ^{++} production which increases from 29% at 8 GeV/c to 35% at 16 GeV/c. The resonance production in the studied reaction is dominated by a single ρ^0 contribution of 55–60% whereas about 16% of all events reveal double ρ^0 production yielding an average ρ^0 multiplicity of 0.9 at both energies.

It should be mentioned that at 8 GeV/c all ρ^0 resonances seem to be centrally produced whereas at 16 GeV/c about $\frac{1}{5}$ of the ρ^0 resonances is directly correlated with the incident pion in the sense that it enters the leading particle function $\psi_2^a(\pi^+\pi^-)$ (table 2). Naturally this difference is not too significant because of the smallness of the t cutoff parameter d_2 for mesons (table 1).

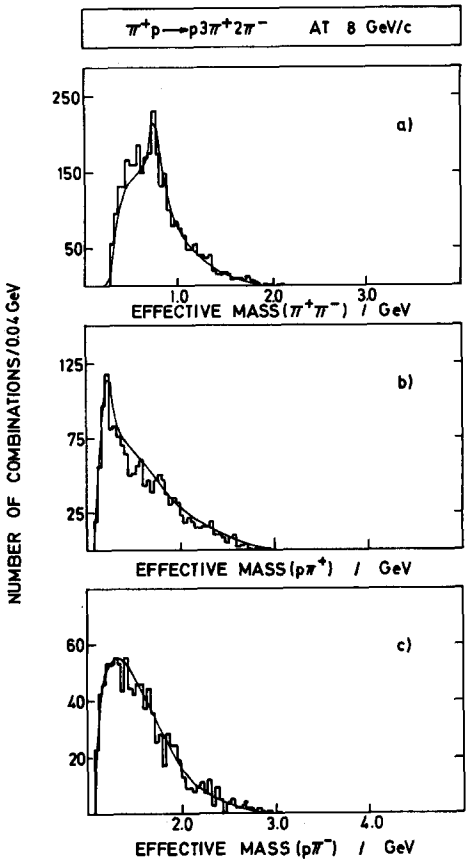

Fig. 4. Two-particle mass distribution for $(\pi^+\pi^-)$, $(p\pi^+)$, $(p\pi^-)$ at 8 GeV/c, and CJM curve.

3.3. Description of three-particle distributions

Since we have neglected in the present version of the CJM three- and more-particle dynamical correlations, $\varphi_m(m \geqslant 3)$, the description of three-particle distributions becomes a critical test of the model. For example in fig. 5 the experimental $(\pi^+\pi^+\pi^-)$ and $(p\pi^+\pi^-)$ mass distributions at 16 GeV/c are given which are well represented by the CJM curves. We remark that these distributions were not used to fit the parameters of the model. For a comparison the curves of the UJM, with the same normalization as in the two-particle distributions, are shown. Moreover, it is interesting to look for the influence of the different reaction channels to the net shape of the distributions. The model curves corresponding to the most interesting channels are shown in figs. 6 and 7. For instance in the case of the 3π mass distribution (fig. 6) the main contributions to the peak in the A resonance region

Table 2
Relative amounts of the different reaction channels contributing to the model amplitude squared $|T|^2$

PARTICLES IN FINAL STATE	8 GeV/c		16 GeV/c	
	relative amounts/%		relative amounts/%	
$\pi^+\|2\pi^+2\pi^-\|p$	69.8 ± 10.0	12.8 ± 1.0	52.4 ± 7.7	11.8 ± 1.0
$\pi^+\|\pi^+\pi^-\rho^0\|p$		41.1 ± 5.0		31.0 ± 4.7
$\pi^+\|2\rho^0\|p$		15.9 ± 4.0		9.6 ± 2.0
$\rho^0\|2\pi^+\pi^-\|p$	-	-	10.9 ± 3.0	5.3 ± 1.0
$\rho^0\|\pi^+\rho^0\|p$		-		5.6 ± 2.0
$\pi^+\|\pi^+2\pi^-\|\Delta^{++}$	29.2 ± 3.0	12.0 ± 1.0	28.2 ± 2.6	13.9 ± 0.6
$\pi^+\|\pi^-\rho^0\|\Delta^{++}$		17.2 ± 2.0		14.3 ± 2.0
$\rho^0\|\pi^+\pi^-\|\Delta^{++}$	-	-	6.6 ± 1.2	4.6 ± 0.7
$\rho^0\|\rho^0\|\Delta^{++}$		-		2.0 ± 0.5
$\pi^+\|2\pi^+\pi^-\|\Delta^0$	1.0 ± 0.5	0.4 ± 0.2	1.8 ± 1.0	0.8 ± 0.4
$\pi^+\|\pi^+\rho^0\|\Delta^0$		0.6 ± 0.3		1.0 ± 0.6
$\rho\|\pi^+\pi^+\|\Delta^0$	-	-	0.1 ± 0.1	0.1 ± 0.1

The symbolic notation e.g. $\rho^0|\pi^+\rho^0|p$ means $\psi_2^a(\pi^+\pi^-)\,\varphi_1(\pi^+)\,\varphi_2(\pi^+\pi^-)\,\psi_1^b(p)$.

arise from terms with double ρ^0 production (6e) and single ρ^0 production (6c, f). Pure uncorrelated production of pions (6b) and Δ^{++} production without ρ^0 (6d) give flat distributions with maxima at about 1.6 GeV/c. Therefore in this model the peak in the A region arises from contributions in which the three observed pions consist of an uncorrelated pair of ρ^0 and π^+. Note that the uncorrelated jet model which has only the possibility of three uncorrelated pions $\pi^+\pi^+\pi^-$ is not able to reproduce this peak. Similar conclusions for the $p\pi^+\pi^-$ distribution can be drawn from fig. 7.

If we take into account dynamical three-particle correlations by a function φ_3 we

Table 3
Production of resonances per event at 8 and 16 GeV/c in the reaction $\pi^+p \to p3\pi^+2\pi^-$

PRODUCTION OF RESONANCES/EVENT	8 GeV/c	16 GeV/c	16 GeV/c [12]
Δ^{++}	0.29 ± 0.03	0.35 ± 0.04	0.39 ± 0.02
Δ^{0}	0.01 ± 0.01	0.02 ± 0.01	0.02 ± 0.01
SINGLE ρ^0	0.59 ± 0.07	0.56 ± 0.09	0.77 ± 0.03
DOUBLE ρ^0	0.16 ± 0.04	0.17 ± 0.04	

get for the three-particle distribution besides a part proportional to φ_3 containing genuine three-particle resonances, many other parts factorizing into two functions one of which has a two-particle resonance structure. These latter ones would have also a peak in the A region and, because of the strong two-particle resonance produc-

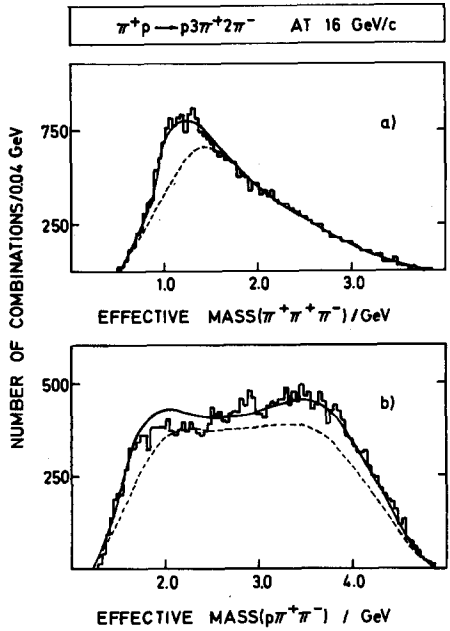

Fig. 5. ($\pi^+\pi^+\pi^-$) and ($p\pi^+\pi^-$) mass distributions at 16 GeV/c. Solid curve: CJM; dashed curve: UJM with the normalization fixed in fig. 3a.

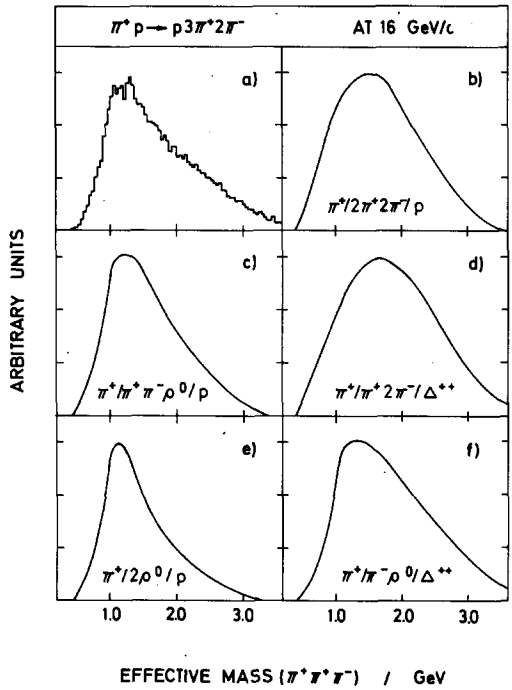

Fig. 6. Experimental $(\pi^+\pi^+\pi^-)$ mass distribution at 16 GeV/c and CJM curves for characteristic reaction channels normalized to the maximum of the experimental distribution (the symbolic notation e.g. $\pi^+|\pi^-\rho^0|\Delta^{++}$ means $\psi_1^a(\pi^+)\varphi_1(\pi^-)\varphi_2(\pi^+\pi^-)\psi_1^b(p\pi^+)$).

tion, yield an important contribution to three-particle distributions. They must always be subtracted before estimating genuine three-particle resonance effects.

From the model calculations with $\varphi_3 = 0$ we find here that the two-particle resonance effects (and the pure uncorrelated production) are sufficient to describe three-particle mass distributions. Naturally, in reactions with a π^0 in the final state one should include three-particle resonances as the ω.

3.4. Azimuthal correlations

The presented version of the CJM consists of an approximation of dynamical correlations by two-particle resonances. Hence it is evident that especially the two-particle mass distributions are quite well represented whereas it is not *a priori* clear that azimuthal angular correlation effects [1] can be described in this way. Furthermore, they seem to be suitable to discriminate between different models [11]. Especially for the multiperipheral model the results are embarrasing as emphasized in ref. [12].

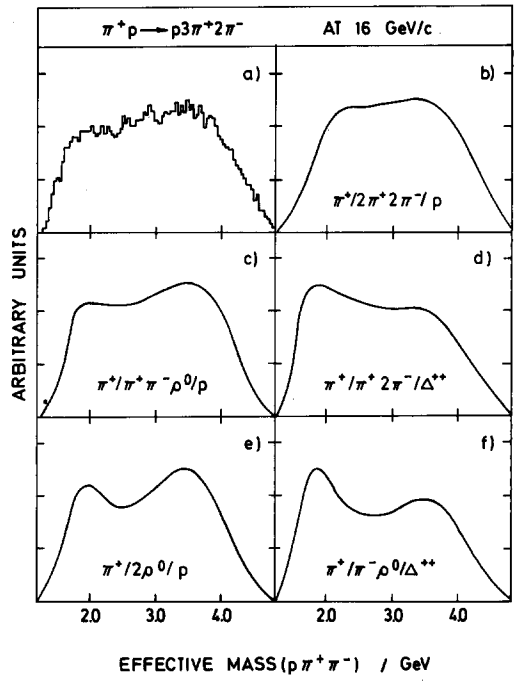

Fig. 7. Experimental ($p\pi^+\pi^-$) mass distribution at 16 GeV/c and CJM curves for characteristic reaction channels normalized to the maximum of the experimental distribution (labelling of reaction channels as in fig. 6).

The two-particle distribution depending on the azimuthal angle can be represented by the series

$$\frac{d\sigma}{d\phi} = \sum_{m=0}^{\infty} A_m \cos m\phi ,$$

with $\cos\phi = \boldsymbol{p}_{i\perp} \cdot \boldsymbol{p}_{j\perp}/|\boldsymbol{p}_{\perp i}|\,|\boldsymbol{p}_{\perp j}|$. The calculation of the mean value of $\cos\phi$ yields the coefficient $A_1/2A_0$. If the remaining coefficients A_n for $n \geqslant 2$ are negligible, as in the uncorrelated jet model, $\langle\cos\phi\rangle$ can be approximated by $-\frac{1}{4}\pi B$ where B is the often used forward-backward asymmetry ratio.

Fig. 8 shows the experimental and model values of $\langle\cos\phi\rangle$ as a function of the absolute rapidity difference of like (fig. 8a) and unlike (fig. 8b) charged pions at 16 GeV/c. Additionally the UJM curve is given (dashed curves in fig. 8) which does not describe the experimental values. For a comparison with semi-inclusive and inclusive data of π^-p reactions at 40 GeV/c lab momentum, see ref. [11]. As in this work, we also find a characteristic short range effect for the unlike charged pion combination. Both experimental distributions are rather well described by the CJM.

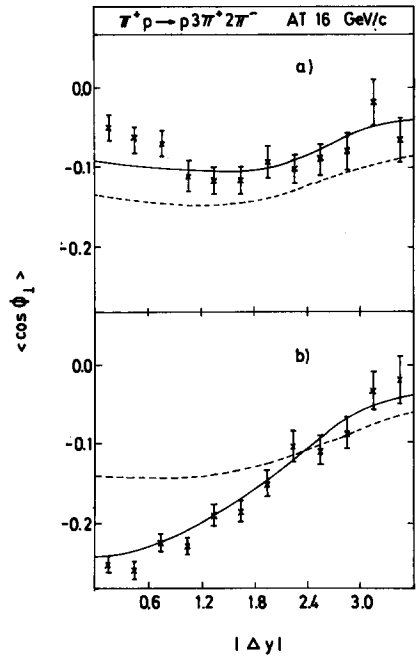

Fig. 8. Mean value of cos ϕ of the azimuthal angle at 16 GeV/c as a function of the rapidity difference for like (8a) and unlike (8b) charged pions. Solid curve: CJM; (dashed curve: UJM.

Here we explain the short range effect for $\pi^+\pi^-$ mainly by the ρ^0 resonance decay into the observed π^+ and π^- mesons. It contributes dominantly only for small rapidity differences. Since we have a transverse momentum cutoff for the $p_\perp$ of the ρ^0 meson in $\varphi_2(\pi^+\pi^-)$ [eq. (2.9)] and momentum conservation for the ρ^0 decay, $p_\perp(\rho^0) = p_\perp(\pi^+) + p_\perp(\pi^-)$, the two pions are produced most frequently with opposite transversal momenta yielding the strong negative azimuthal correlations. Note that a separate $p_\perp$ cutoff as in the product $\varphi_1(\pi^+) \cdot \varphi_1(\pi^-)$ for both mesons coming from the resonances does not lead to this result. Besides this dynamical short-range effect due to resonance decay we have additionally a kinematical long-range effect because of overall transverse momentum conservation. Similar conclusions are obtained also in ref. [13] for inclusive correlations at ISR energies.

The influence of different resonances on the azimuthal correlations can be studied by looking e.g. for the cos ϕ mean values integrated over Δy for the different reaction channels given in table 4. Comparing channels with a different number of ρ^0 (whether leading or not) but equal baryons we see that with an increasing number of ρ^0 the values of $-\langle \cos \phi \rangle$ increase for $\pi^+\pi^-$ as expected, but even decrease for $\pi^\pm\pi^\pm$ as a compensation effect. Transverse momentum conversation sum rules relate the two-particle distributions $\sigma_2(i, j)$ of a given particle i to all other particles j, i, j = π^+, π^-, p. Therefore a dynamical increase of the (negative) $\pi^+\pi^-$ azimuthal correlations reduces

Table 4
Experimental and theoretical mean values of cos ϕ of the azimuthal angle of like and unlike charged pions at 16 GeV/c

PARTICLES IN FINAL STATE	RELATIVE AMOUNT/%	$-\langle\cos\phi\rangle_{\pi^\pm\pi^\pm}$	$-\langle\cos\phi\rangle_{\pi^+\pi^-}$
$\pi^+\|2\pi^+2\pi^-\|p$	11.8	0.134	0.147
$\pi^+\|\pi^+\pi^-\rho^0\|p$ $\rho^0\|2\pi^+\pi^-\|p$	36.3	0.093	0.182
$\pi^+\|\ 2\rho^0\ \|p$ $\rho^0\|\pi^+\rho^0\ \|p$	15.2	0.068	0.208
$\pi^+\|\pi^+2\pi^-\|\Delta^{++}$	13.9	0.138	0.127
$\pi^+\|\ \pi^-\rho^0\ \|\Delta^{++}$ $\rho^0\|\pi^+\pi^-\|\Delta^{++}$	18.9	0.112	0.155
$\rho^0\|\ \rho^0\ \ \|\Delta^{++}$	2.0	0.073	0.218
$\pi^+\|2\pi^+\pi^-\|\Delta^0$	0.8	0.133	0.129
$\pi^+\|\ \pi^+\rho^0\ \|\Delta^0$ $\rho^0\|\ 2\pi^+\ \|\Delta^0$	1.1	0.036	0.159
ALL		0.103	0.170
EXPERIMENT		0.082±0.005	0.191±0.004

Labelling of reaction channels as in table 2.

automatically the correlations for $\pi^\pm\pi^\pm$. The difference between like and unlike charged pion combinations is rather impressive for double ρ^0 production. On the other hand, keeping the number of ρ^0 fixed and comparing channels with different leading baryons we find that Δ production generally suppresses the negative azimuthal correlation effect for $\pi^+\pi^-$ (with the exception of the $\rho^0/\rho^0/\Delta^{++}$ channel). For like charged pions we find an enhancement from Δ^{++} and a suppression from ρ^0 as compared to leading protons. The weighted sum of all 12 contributions, $\langle\cos\phi\rangle = -0.170$,

is close to the experimental value of -0.191 for $\pi^+\pi^-$. For like charged pions the resonance effect reduces the value of $-\langle\cos\phi\rangle$ from 0.134 of the UJM to 0.103 which is in the right direction to the experimental value 0.082. A better agreement could be achieved by slightly different weights of the various contributions, especially with somewhat stronger double ρ^0 and/or Δ^0 production. Note that, as for the three-particle distributions, the azimuthal correlations where not used for the fit of the parameters of the model. More details on the azimuthal correlations with curves for the ϕ dependence will be given in a forthcoming paper.

4. Summary

The aim of the present analysis was to test the applicability of the correlated jet model (CJM) to an exclusive multi-particle reaction at two medium energies incorporating for the dynamical two-particle correlation function in the amplitude squared resonance effects only. From the comparison of the model with the data of the reaction $\pi^+p \to p3\pi^+2\pi^-$ at 8 and 16 GeV/c we found:

(i) The CJM fits well to the one- and two-particle distributions considered.

(ii) The results are consistent with the assumption of an energy independent central part of particle production within the regarded energy range.

(iii) Taking into account both kinematics and effects of the reflection of resonances of other reaction channels, the relative amounts of the dominant two-particle resonances included in the amplitude squared are quoted (table 2).

(iv) Three-particle mass distributions are represented quite well by the CJM although dynamical three-particle correlations are not included. Therefore it should be emphasized that the study of genuine three-particle resonances requires to take into account the important influence of two-particle resonances.

(v) The behaviour of azimuthal correlation parameters in the studied exclusive reaction is similar to the semi-inclusive and inclusive cases. It especially reveals an important short range effect for unlike charged pion combinations. The mean values of $\cos\phi$ of the azimuthal angle are well reproduced by the CJM and can be explained by the influence of resonances produced with a cutoff in the sum of the transverse momenta of the particles into which the resonances decay.

The authors would like to thank the ABBCCHW collaboration for permission to use the 8 and 16 GeV/c π^+p data and for interesting discussions with D.R.O. Morrison and S. Humble. We also are indebted to D. Ebert, E.H. de Groot, U. Kundt, K. Lanius, H. Miettinen, H.B. Nielsen, and P. Olesen for many valuable discussions and suggestions.

References

[1] J. Ranft, Proc. 5th Int. Symp. on many-particle hadrodynamics, Eisenach-Leipzig, 1974; K. Zalewski, Proc. 17th Int. Conf. on high-energy physics, London, 1974.

[2] S. Pokorsky and L. Van Hove, Acta Phys. Pol. B5 (1974) 229.
[3] K.J. Biebl, A.correlated jet model for multi-particle production, Berlin preprint PHE 75-2 (1975).
[4] E.H. de Groot, Nucl. Phys. B48 (1972) 259;
D. Sivers and G.M. Thomas, Phys. Rev. D6 (1972) 1961.
[5] K.G. Wilson, Cornell preprint CLNS-131 (1970) unpublished;
A.H. Mueller, Phys. Rev. D4 (1971) 160.
[6] P. Olesen, Nucl. Phys. B47 (1972) 157.
[7] F. Hayot and M. Le Bellac, preprint UM-HE-74-7 (1974);
J.W. Dash, J. Huskins and S.T. Jones, ANL/HEP 7355 (1973).
[8] K.J. Biebl., D. Bebel and D. Ebert, Fortschr. der Phys. 20 (1972) 541.
[9] H. Böttcher, K. Lanius and CH. Spiering, Berlin preprint PHE 74-2 (1974).
[10] F. James, CERN Program Library W 505 (1968).
[11] G. Ranft and J. Ranft, Leipzig preprint KMU-HEP-7410 (1974);
R. Blutner et al., Leipzig preprint KMU-HEP-7404 (1974);
G. Ranft and J. Ranft, Phys. Letters 53B (1974) 188.
[12] J.H. Friedman, C. Risk and D.B. Smith, Phys. Rev. Letters 28 (1972) 191.
[13] K. Eggert et al., Nucl. Phys. B86 (1975) 201.
[14] D. Sivers and G.H. Thomas, Phys. Rev. D7 (1973) 516.